HHS Public Access

Author manuscript

Clin Cancer Res. Author manuscript; available in PMC 2023 January 24.

Published in final edited form as:

Clin Cancer Res. 2018 July 15; 24(14): 3366–3376. doi:10.1158/1078-0432.CCR-17-2483.

The RNA-binding Protein MEX3B Mediates Resistance to Cancer Immunotherapy by Downregulating HLA-A Expression

Lu Huang[1], **Shruti Malu**[1], **Jodi A. McKenzie**[1], **Miles C. Andrews**[2], **Amjad H. Talukder**[1], **Trang Tieu**[3], **Tatiana Karpinets**[4], **Cara Haymaker**[1], **Marie-Andrée Forget**[1], **Leila J. Williams**[1], **Zhe Wang**[1], **Rina M. Mbofung**[1], **Zhi-Qiang Wang**[5], **Richard Eric Davis**[5], **Roger S. Lo**[6], **Jennifer A. Wargo**[2], **Michael A. Davies**[1], **Chantale Bernatchez**[1], **Timothy Heffernan**[3], **Rodabe N. Amaria**[1], **Anil Korkut**[7], **Weiyi Peng**[1], **Jason Roszik**[1], **Gregory Lizée**[1], **Scott E. Woodman**[1], **Patrick Hwu**[1]

[1]Department of Melanoma Medical Oncology, The University of Texas MD Anderson Cancer Center, Houston, Texas.

[2]Department of Surgical Oncology, The University of Texas MD Anderson Cancer Center, Houston, Texas.

[3]Institute for Applied Cancer Science, The University of Texas MD Anderson Cancer Center, Houston, Texas.

[4]Department of Genomic Medicine, The University of Texas MD Anderson Cancer Center, Houston, Texas.

[5]Department of Lymphoma/Myeloma, The University of Texas MD Anderson Cancer Center, Houston, Texas.

[6]Department of Medicine, The University of California, Los Angeles, Los Angeles, California.

[7]Department of Bioinformatics and Computational Biology, The University of Texas MD Anderson Cancer Center, Houston, Texas.

Corresponding Author: Patrick Hwu, The University of Texas MD Anderson Cancer Center, 1515 Holcombe Boulevard, Unit 0421, Houston, TX 77030. Phone: 713-563-1727; Fax: 713-792-4654, phwu@mdanderson.org.

Current address for S. Malu: Eli Lilly and Company, Lilly Corporate Center, Indianapolis, Indiana.

Authors' Contributions

Conception and design: L. Huang, S. Malu, W. Peng, P. Hwu

Development of methodology: L. Huang, S. Malu, A.H. Talukder, T.P. Heffernan, S.E. Woodman

Acquisition of data (provided animals, acquired and managed patients, provided facilities, etc.): L. Huang, S. Malu, J.A. McKenzie, M.C. Andrews, C. Haymaker, M.-A. Forget, L.J. Williams, Z. Wang, R. Mbofung, Z.-Q. Wang, R.S. Lo, J.A. Wargo, G. Lizee

Analysis and interpretation of data (e.g., statistical analysis, biostatistics, computational analysis): L. Huang, S. Malu, T.V. Karpinets, R.N. Amaria, A. Korkut, W. Peng, J. Roszik, G. Lizee, S.E. Woodman, P. Hwu

Writing, review, and/or revision of the manuscript: L. Huang, J.A. McKenzie, M.C. Andrews, C. Haymaker, M.-A. Forget, Z. Wang, R.E. Davis, R.S. Lo, J.A. Wargo, M.A. Davies, R.N. Amaria, W. Peng, J. Roszik, G. Lizee, S.E. Woodman, P. Hwu

Administrative, technical, or material support (i.e., reporting or organizing data, constructing databases): L. Huang, A.H. Talukder, R.S. Lo, J.A. Wargo, C. Bernatchez, P. Hwu

Study supervision: S.E. Woodman, P. Hwu

Other (molecular biology support with construct design, cloning, and library generation): T. Tieu

Disclosure of Potential Conflicts of Interest

No potential conflicts of interest were disclosed.

Note: Supplementary data for this article are available at Clinical Cancer Research Online (http://clincancerres.aacrjournals.org/).

Abstract

Purpose: Cancer immunotherapy has shown promising clinical outcomes in many patients. However, some patients still fail to respond, and new strategies are needed to overcome resistance. The purpose of this study was to identify novel genes and understand the mechanisms that confer resistance to cancer immunotherapy.

Experimental Design: To identify genes mediating resistance to T-cell killing, we performed an open reading frame (ORF) screen of a kinome library to study whether overexpression of a gene in patient-derived melanoma cells could inhibit their susceptibility to killing by autologous tumor-infiltrating lymphocytes (TIL).

Results: The RNA-binding protein MEX3B was identified as a top candidate that decreased the susceptibility of melanoma cells to killing by TILs. Further analyses of anti–PD-1–treated melanoma patient tumor samples suggested that higher *MEX3B* expression is associated with resistance to PD-1 blockade. In addition, significantly decreased levels of IFNγ were secreted from TILs incubated with MEX3B-overexpressing tumor cells. Interestingly, this phenotype was rescued upon overexpression of exogenous HLA-A2. Consistent with this, we observed decreased HLA-A expression in MEX3B-overexpressing tumor cells. Finally, luciferase reporter assays and RNA-binding protein immunoprecipitation assays suggest that this is due to MEX3B binding to the 3′ untranslated region (UTR) of *HLA-A* to destabilize the mRNA.

Conclusions: MEX3B mediates resistance to cancer immunotherapy by binding to the 3′ UTR of *HLA-A* to destabilize the *HLA-A* mRNA and thus downregulate HLA-A expression on the surface of tumor cells, thereby making the tumor cells unable to be recognized and killed by T cells.

Introduction

In the past few years, significant progress has been made in the field of cancer immunotherapy, which seeks to use the body's own immune system to fight cancer (1). Blocking antibodies against the immune checkpoint molecules CTLA-4 and PD-1 as well as T-cell therapy using autologous tumor-infiltrating lymphocytes (TIL) or T-cell receptor (TCR)–modified T cells have led to promising and durable clinical outcomes in various types of cancer (1–9). However, these durable responses are only achieved in a subset of patients, and currently there is very limited ability to predict whether a patient is likely to respond to immunotherapy (1, 4, 6). An improved understanding of the underlying molecular mechanisms of tumor resistance to immunotherapy in nonresponders will facilitate the development of (i) biomarkers that can predict whether a patient is likely to benefit from immunotherapy at the time of treatment initiation and (ii) more effective therapeutic strategies that target genes mediating immunoresistance in combination with immunotherapy. Both of these advances will help improve patient outcomes.

Recently, several studies have elucidated some tumor-intrinsic molecular mechanisms of resistance to immunotherapy. For example, loss of the tumor suppressor gene *PTEN* has been found to be correlated with poor outcomes in patients with melanoma treated with anti–PD-1 (10), and aberrations in the IFN signaling pathway have been shown to be associated with primary resistance to anti–CTLA-4 therapy (11). Furthermore, analysis

of tumors from patients with melanoma who progressed after initially responding to anti–PD-1 therapy revealed that acquired resistance to anti–PD-1 was associated with mutations in genes involved in interferon receptor signaling and antigen presentation (12). Finally, activation of Wnt/β-catenin signaling in tumor cells has been shown to be associated with a non–T-cell–inflamed state in melanoma and to correlate with resistance to checkpoint blockade in preclinical models (13).

To identify additional genes that may confer resistance to immunotherapy in an unbiased fashion, we performed an open reading frame (ORF) screen focusing on T-cell–induced apoptosis (killing) of tumor cells, also referred to as T-cell–mediated cytotoxicity. The screen identified MEX3B as a candidate whose overexpression in melanoma cells decreased their susceptibility to killing by autologous TILs *in vitro*, suggesting that MEX3B may confer resistance to cancer immunotherapy.

MEX3B is part of the MEX3 (muscle excess 3) family of translational regulators (14). It is an RNA-binding protein that binds to RNA through two KH domains (14). MEX3B destabilizes its own mRNA by binding to the 3′ long conserved untranslated region [UTR (3′ LCU)], which contains elements for mRNA destabilization and translational enhancement (15). The function of MEX3B in immune responses has not been well studied, although one study showed that MEX3B can act as a coreceptor of TLR3 in the innate antiviral response (16, 17). However, the role of MEX3B in T-cell–mediated antitumor immune responses remains unclear. This study investigated the role of MEX3B in resistance to immunotherapy using melanoma as a model, which so far has shown the best clinical outcomes to cancer immunotherapy. We found that overexpression of MEX3B in melanoma cells can downregulate the expression of HLA-A by binding to the 3′ UTR of *HLA-A* mRNA, thereby blocking the recognition and killing of tumor cells by T cells and mediating resistance to immunotherapy.

Materials and Methods

Cell lines

The human melanoma cell lines and TILs used for this study were derived from tumor tissue obtained from patients with metastatic melanoma enrolled in an adoptive cell therapy clinical trial using TILs at The University of Texas MD Anderson Cancer Center (MDACC, Houston, TX). The trial was performed under an institutional review board–approved protocol (#2004–0069, NCT00338377) and in compliance with Good Clinical Practice concerning medical research in humans, as described in the Declaration of Helsinki. All patients granted written informed consent. Melanoma TILs were generated as previously described (6, 18). All tumor cell lines were maintained in complete cell culture medium as described previously (10) and were authenticated using short tandem repeat (STR) DNA fingerprinting performed at the Characterized Cell Line Core Facility at MDACC. All cell lines were tested by a *Mycoplasma* testing kit (Lonza, catalog number LT07–418) to ensure they were *Mycoplasma* negative before being used for any experiments.

Lentiviral particles containing EGFP or EGFP and ORFs were produced as previously described using pHAGE-EF1α-IRES-EGFP lentiviral vector (10). Patient-derived melanoma

cells were infected with these lentiviruses, and stable cell lines were generated by sorting for GFP-positive cells after viral transduction. Lentiviral particles containing shRNAs were produced as previously described using pLKO.1-puro vector (10). Patient-derived melanoma cells were infected with these lentiviruses, and stable cell lines were generated by puromycin selection. Established cell lines were subsequently used for *in vitro* experiments.

ORF screen and T-cell–mediated cytotoxicity assay

The patient-derived melanoma cell line 2549 was screened using a kinome library of 384 gene ORFs (Life Technologies). Tumor cells were plated at 5×10^4 cells per well in 96-well plates. Each well of cells was infected with lentiviral particles containing GFP only or GFP plus one gene ORF. Three days after transduction, tumor-reactive autologous TILs were added to the target tumor cells at predetermined effector (TIL) to target cell (tumors) ratios (E:T ratios) and incubated at 37°C for 3 hours. Cells were then fixed with fixation/permeabilization solution (BD Biosciences, catalog number 554714) and stained for activated caspase-3 (using anti-cleaved caspase-3 antibody; BD Biosciences, catalog number 550821), followed by flow cytometry in 96-well plates. The percentage of activated caspase-3–positive tumor cells was used as a readout for apoptosis of tumor cells mediated by TILs (19). Tumor cells that were not incubated with any TILs were also assessed. A "comboscore" was then used to evaluate the effect of the combination of each ORF and TILs. The comboscore was calculated using the following formula: $[(\text{Apoptosis}_{ORF+TILs} - \text{Apoptosis}_{ORF})/(\text{Apoptosis}_{GFP+TILs} - \text{Apoptosis}_{GFP})]^2$. A comboscore of less than 1 was indicative of resistance to T-cell–mediated cytotoxicity.

For T-cell–mediated cytotoxicity assay on established stable cell lines, tumor-reactive autologous TILs were added to the target tumor cells (5×10^4 cells per well in 96-well plates) at different E:T ratios and incubated at 37°C for 3 hours. If the tumor cells did not express GFP (in the case of tumor cells expressing shRNA), they were first labeled with DDAO cell tracker dye before being plated in 96-well plates. After 3-hour tumor–TIL incubation, cells were fixed and stained for activated caspase-3, followed by flow cytometry to analyze the percentage of activated caspase-3–positive tumor cells as a readout for apoptosis of tumor cells mediated by TILs. The representative flow gating strategy is shown in Supplementary Fig. S1.

ELISA

Tumor-reactive TILs were added to the target tumor cells (5×10^4 cells per well in 96-well plates) at different E:T ratios and incubated at 37°C for 24 hours. When MART-1–specific TILs were used, tumor cells were first pulsed with MART-$1_{26–35}$ peptide (ELAGIGILTV) by incubating them with 1 mmol/L MART-1 peptide in Opti-MEM at 37°C for 1 hour. Supernatants were collected and frozen at −80°C until ready for analysis. ELISA to measure IFNγ levels was performed using a kit according to the manufacturer's manual (eBioscience, catalog number 88–7316-88).

Flow cytometry

Melanoma cells were treated with or without human recombinant IFNγ (R&D Systems, 1,000 U/mL) for 24 hours and stained with HLA-A2; HLA-A31; pan-HLA-A/B/C;

HLA-B; or HLA-C antibodies. 2559 melanoma cells were stained with Alexa Fluor 647–conjugated mouse anti-human HLA-A2 antibody (Bio-Rad Laboratories, product code MCA2090A647). 2549 melanoma cells were stained with biotin-conjugated HLA class 1 antigen A30,A31 antibody (United States Biological, catalog number H6098–37A), followed by Alexa Fluor 647–conjugated streptavidin secondary antibody (Thermo Fisher Scientific, catalog number S21374). Both cell lines were stained with PE/Cy7-conjugated anti-human pan-HLA-A/B/C antibody (BioLegend, catalog number 311430), rabbit anti–HLA-B antibody (Invitrogen, catalog number PA5–35345) followed by Alexa Fluor 568–conjugated goat anti-rabbit IgG secondary antibody (Invitrogen, catalog number A-11036), or mouse anti–HLA-C antibody (Novus Biologicals, catalog number NBP2–50419) followed by Alexa Fluor 568–conjugated goat anti-mouse IgG secondary antibody (Invitrogen, catalog number A-21124). Stained samples were acquired on a BD LSRFortessa instrument and data analyzed using FlowJo software.

Quantitative real-time PCR

Total RNA was extracted using RNeasy plus mini kit (QIAGEN). Two micrograms of RNA were reverse transcribed to cDNA using the High Capacity RNA-to-cDNA kit (Thermo Fisher Scientific). Quantitative real-time PCR (qRT-PCR) was performed using the TaqMan gene expression assay system (Life Technologies). The following assay IDs were used: GAPDH (Hs02786624_g1), MEX3B (Hs00863082_m1), HLA-A (Hs01058806_g1), B2M (Hs00187842_m1), TAP1 (Hs00388675_m1), TAP2 (Hs00241260_m1), TAPBP (Hs00917451_m1), CALR (Hs00189032_m1), CANX (01558409_m1), PSMB8 (Hs00544758_m1), and PSMB9 (Hs00160610_m1). Samples were normalized to GAPDH expression level using $2^{-\Delta\Delta C_t}$ method.

Dual-luciferase reporter assay

293 T cells were plated at 3×10^4 cells per well in 96-well plates. The next day, each well of cells was transfected with 300 ng pGL3 [expressing firefly luciferase (ffLuc)] or pGL3-HLA-A2 3′UTR (kindly provided by Dr. Paul Lehner from University of Cambridge, Cambridge, United Kingdom), 300 ng pHAGE-EF1α-IRES-EGFP or pHAGE-EF1α-IRES-EGFP-MEX3B, and 1 ng control pRL-TK plasmid (expressing *Renilla* luciferase as a control for transfection efficiency). Each combination of plasmids was transfected in triplicates. Two days after transfection, dual-luciferase reporter assay was performed using Dual-Luciferase reporter assay system (Promega, catalog number E1910) according to the manufacturer's manuals. The ffLuc activity was first normalized to the *Renilla* luciferase activity in each sample. The relative luciferase activity in cells transfected with pGL3-HLA-A2 3′ UTR and pHAGE-EF1a-IRES-EGFP was normalized to those transfected with pGL3 and pHAGE-EF1α-IRES-EGFP. Similarly, the relative luciferase activity in those transfected with pGL3-HLA-A2 3′ UTR and pHAGE-EF1α-IRES-EGFP-MEX3B was normalized to those transfected with pGL3 and pHAGE-EF1α-IRES-EGFP-MEX3B.

Alternatively, each well of 293 T cells was transfected with 300 ng pGL3 or pGL3-HLA-A2 3′UTR, 300 ng pCDNA3.1, pCDNA3.1-MEX3B (wild type), or pCDNA3.1-MEX3B-mutKH (kindly provided by Dr. Tetsu Akiyama from University of Tokyo, Tokyo, Japan) and 1 ng control pRL-TK plasmid. Dual-luciferase reporter assay was performed and data

analyzed similarly. The relative luciferase activity in cells transfected with pGL3-HLA-A2 3′ UTR and pCDNA3.1 was normalized to those transfected with pGL3 and pCDNA3.1. Similarly, the relative luciferase activity in cells transfected with pGL3-HLA-A2 3′ UTR and pCDNA3.1-MEX3B was normalized to those transfected with pGL3 and pCDNA3.1-MEX3B, and the relative luciferase activity in cells transfected with pGL3-HLA-A2 3′ UTR and pCDNA3.1-MEX3B-mutKH was normalized to those transfected with pGL3 and pCDNA3.1-MEX3B-mutKH.

RNA-binding protein immunoprecipitation assay

An RNA-binding protein immunoprecipitation (RIP) assay was performed on melanoma cells using RIP kit from EMD Millipore (catalog number 17–701). Cell lysates were immunoprecipitated with anti-mouse monoclonal MEX3B (4C4) antibody from Santa Cruz Biotechnology (catalog number sc-293407) or mouse IgG as a control. Coimmunoprecipitated RNA was recovered, and qRT-PCR was performed as described above to amplify *HLA-A*. MEX3B-associated *HLA-A* levels were normalized to control mouse IgG–associated *HLA-A* levels using $2^{-\Delta Ct}$ method.

Analysis of patient datasets

The publicly available The Cancer Genome Atlas (TCGA) database for skin cutaneous melanoma was used as a source for melanoma patient data (20). Analyses included mRNA expression [RNA sequencing (RNA-Seq)] and lymphocyte score (pathology review).

The RNA-Seq data from patients with melanoma treated with anti–PD-1 were derived from a published dataset (21). The RNA expression values of *MEX3B* and *HLA-A* from 15 responders and 13 nonresponders were compared using the standard score (Z value). To calculate the score, we log-transformed Fragments Per Kilobase of transcript per Million mapped reads (FPKM) values of the genes and calculated their mean (X_{mean}) and standard deviation (X_{stdev}). We used the values to calculate the Z score for each sample as $(X\text{-}X_{mean})/X_{stdev}$, where X is the log-transformed FPKM value of the gene in the sample. The *MEX3B* Z scores of the samples were ranked from the highest to the lowest and represented in gradually changing colors. These Z scores were also plotted using GraphPad Prism. The association between *MEX3B* and *HLA-A* Z scores was analyzed using Spearman correlation coefficient and *P* values.

Patient sample collection and analysis

Analysis of *MEX3B* expression in an anti–PD-1–treated patient cohort at MDACC was performed under institutional review board–approved protocols (PA12–0875, 2012–0846, LAB00–063, PA12–0305, and PA15–0232) and in compliance with Good Clinical Practice concerning medical research in humans, as described in the Declaration of Helsinki. All patients granted written informed consent. Fourteen patients with melanoma treated with anti–PD-1 immunotherapy who had pretreatment tumor biopsies were identified by the Melanoma Core Lab at MDACC, and RNA was extracted from these pre-anti–PD-1 tumor FFPE blocks. Another 13 RNA samples from pre-anti–PD-1–treated patient tumors were obtained from a previous cohort under the APOLLO (Adaptive Patient-Oriented Longitudinal Learning and Optimization) platform at MDACC. qRT-PCR for *MEX3B* and

GAPDH was performed as described above. The best response of each patient to anti–PD-1 immunotherapy was determined by a medical oncologist using RECIST 1.1 criteria.

Statistical analysis

For the analysis of the correlation between *MEX3B* and *CD8A* or *HLA-A* in the TCGA melanoma database, the mRNA expression [Transcripts Per Kilobase Million (TPM)] of *MEX3B* and *CD8A* or *HLA-A*, was log(10)-transformed, which was found to be close to normal distribution. Therefore, the association between *MEX3B* and *CD8A* or *HLA-A* was evaluated using both Pearson and Spearman coefficient, which generated similar results. Pearson coefficients and *P* values were reported.

TCGA data analysis of the correlation of cytolytic score and lymphocyte score with *MEX3B* expression are represented as box and whisker plots generated by Tableau software. All other data are represented as mean ± SEM and generated by GraphPad Prism. Statistical analysis was also performed using GraphPad Prism. Mann–Whitney test or Student *t* test was used for the comparison of continuous variables between two groups. One-way ANOVA plus the Tukey multiple comparisons test was used for the comparison of continuous variables among three groups. Significant differences are indicated by * ($P < 0.05$), ** ($P < 0.01$), *** ($P < 0.001$), or **** ($P < 0.0001$), with $P < 0.05$ as statistically significant.

Results

MEX3B mediates resistance to T-cell–mediated cytotoxicity

To identify potential genes that may confer resistance to T-cell–mediated cytotoxicity in melanoma, we performed an ORF screen on patient-derived human melanoma cells and their autologous TILs. Briefly, melanoma cells were transduced with individual lentiviruses expressing GFP only or GFP plus one of 384 ORFs from a kinome library (Supplementary Table S1), adapted from a previously published kinome library (22) and comprised of a wide cross-section of kinases known to be expressed in human cells. The transduced melanoma cells were incubated with or without autologous TILs, followed by intracellular staining of activated caspase-3, a marker for apoptosis (Fig. 1A). The percentage of activated caspase-3–positive (in GFP positive) melanoma cells was used to indicate the level of apoptosis of melanoma cells. T-cell–mediated cytotoxicity was quantified as the difference in the apoptosis of melanoma cells cocultured with and without TILs. The impact of each ORF on T-cell–mediated cytotoxicity was measured by calculating a comboscore, which is the T-cell–mediated cytotoxicity on ORF-transduced melanoma cells divided by that on GFP-transduced melanoma cells (see “Materials and Methods“ section for the equation). A comboscore of more than 1 suggests higher T-cell–mediated cytotoxicity on ORF-transduced cells than on GFP control cells; a comboscore of less than 1 indicates inhibition of T-cell–mediated cytotoxicity on ORF-transduced cells.

Among the 384 ORFs screened, we identified the top 20 candidates with the highest comboscores (Supplementary Fig. S2) as well as the major pathways these genes are involved in (Supplementary Table S2) by searching in the Pathway Commons database (23). However, as our main purpose of performing the screen was to identify immunoresistance

genes that are targetable, we focused on the top 20 hits with the lowest comboscores (Fig. 1B), indicating their potential to inhibit T-cell–mediated killing of melanoma cells. To determine which of these candidates is most likely to confer resistance to immunotherapy in patients with melanoma, we took advantage of the publicly available RNA-Seq data from a published cohort of patients with melanoma treated with anti–PD-1 antibodies (21). Of these 20 candidates with the lowest comboscores, the RNA-binding protein MEX3B, which ranked 10th lowest of the 384 ORFs (Fig. 1B), was the only candidate that showed significant different expression between responders and nonresponders to anti–PD-1 therapy (Fig. 1C). *MEX3B* mRNA expression in pretreatment tumor samples was significantly higher in nonresponders than in responders to anti–PD-1 (Fig. 1C), indicating a potential role of MEX3B in mediating resistance to immunotherapy. To verify this result, we performed qRT-PCR analysis of *MEX3B* in RNA samples from another cohort of patients with melanoma treated with anti–PD-1. We observed a trend of higher MEX3B expression in nonresponders than in responders to anti–PD-1 (Supplementary Fig. S3). Taken together, these data suggest that higher *MEX3B* expression is correlated with worse response to anti–PD-1 immunotherapy. Therefore, we chose to focus on MEX3B for further study of its role in immunoresistance.

We first analyzed patient profiles from the TCGA skin cutaneous melanoma database and identified inverse associations between the expression of *MEX3B* and two indicators of antitumor immune responses, including the RNA-Seq–based immune cytolytic activity score (24) and the IHC-based lymphocyte score, a semiquantitative measure of the number of lymphocytes in a tumor sample (20). Specifically, the cytolytic score was significantly lower in patients with melanoma exhibiting higher *MEX3B* expression than those with lower *MEX3B* expression (Fig. 1D), and patients with low lymphocyte scores had significantly higher *MEX3B* expression than those with high lymphocyte scores (Fig. 1E). We also found that MEX3B expression was negatively associated with CD8A expression (Fig. 1F), further supporting that MEX3B may have a negative effect on $CD8^+$ lymphocyte infiltration. Taken together, these data suggest an association between *MEX3B* expression and resistance to T-cell–mediated immunotherapy.

To validate that MEX3B mediates resistance to T-cell–mediated cytotoxicity, stable melanoma cell lines with altered MEX3B expression were incubated with autologous TILs at different E:T ratios, and the percentage of melanoma cells with activated caspase-3 was measured as a readout for apoptosis. Overexpression of MEX3B in the patient-derived melanoma cell line 2549, which was validated by qRT-PCR (Fig. 2A), significantly decreased the apoptosis induced by autologous TILs (Fig. 2B). Similar results were also observed when MEX3B was overexpressed in the patient-derived melanoma cell line 2559 (Fig. 2C and D). Consistent with these results, knockdown of MEX3B by shRNA in the same melanoma cell lines (Supplementary Fig. S4A and S4B) significantly increased the tumor apoptosis induced by autologous TILs (Supplementary Fig. S4C and S4D). Taken together, these results support a role for MEX3B in resistance to T-cell–mediated cytotoxicity in melanoma cells.

Overexpression of MEX3B in melanoma cells inhibits IFNγ release from autologous TILs

We then explored the potential mechanisms by which MEX3B decreases T-cell–mediated cytotoxicity on tumor cells. TCR recognition of MHC-I–peptide complexes on the tumor cell surface is a prerequisite for IFNγ secretion and tumor cell killing by T cells. Therefore, secreted IFNγ provides an indication of how well tumor cells are recognized by T cells. To investigate whether MEX3B overexpression in melanoma cells attenuates their recognition by T cells, IFNγ levels were examined in supernatants from autologous TILs incubated with melanoma cells with or without MEX3B overexpression. Overexpression of MEX3B in the patient-derived melanoma cell line 2549 decreased IFNγ levels in supernatants by about 90% (Fig. 3A). Similar results were also observed when MEX3B was overexpressed in melanoma cell line 2559 (Fig. 3B). The association between MEX3B overexpression in melanoma cells and diminished IFNγ release from cocultured autologous TILs suggests a role for MEX3B in attenuating the recognition of tumor cells by T cells.

Downregulation of HLA-A expression on MEX3B-overexpressing melanoma cells is responsible for the decreased IFNγ release from TILs

One potential reason for the attenuated tumor–T-cell recognition is a defect in the antigen-specific TCR–MHC-I–peptide recognition upon overexpression of MEX3B. To test this hypothesis, we first enforced antigen-specific recognition by using the human melanoma tumor antigen MART-$1_{26–35}$ peptide (ELAGIGILTV) with its corresponding antigen-specific T cells (named MART-1–specific TILs) that were previously established. As the MART-1 antigen is HLA-A2 restricted (25), the human melanoma cell line 2549 (HLA-A2 negative) overexpressing GFP-MEX3B (or GFP as a control) was transduced with a lentiviral vector expressing human HLA-A2. Stably transduced cells expressing HLA-A2 were pulsed with the MART-1 peptide prior to coincubation with MART-1–specific TILs, and IFNγ levels in supernatants were measured. In contrast to the results in TILs cocultured with autologous MEX3B-overexpressing 2549 melanoma cells (Fig. 3A), IFNγ levels were similar in the supernatants from MART-1–specific TILs incubated with MART-1–pulsed 2549 GFP HLA-A2 or 2549 GFP-MEX3B HLA-A2 cells (Supplementary Fig. S5). This result indicates that enforced MHC-I–peptide complex expression abolishes the inhibitory effect of MEX3B on tumor–T-cell recognition.

To verify whether a similar phenotype exists in the setting of endogenous HLA-A2 expression, we utilized the 2559 cell line (HLA-A2 positive) to determine the effect of MEX3B on antigen-specific recognition of tumor cells by TILs. 2559 cells overexpressing GFP-MEX3B (or GFP as a control) were pulsed with the MART-1 peptide before incubation with MART-1–specific TILs, and IFNγ levels in supernatants were measured. In contrast to the results from 2549 cells overexpressing exogenous HLA-A2 (Supplementary Fig. S5), IFNγ levels were dramatically decreased in supernatants from MART-1–specific TILs incubated with 2559 cells overexpressing GFP-MEX3B in comparison with those incubated with GFP control cells (Fig. 4A). Interestingly, stable overexpression of exogenous HLA-A2 in GFP-MEX3B–overexpressing or GFP control 2559 cells, followed by pulsing with MART-1 and incubation with MART-1–specific TILs, resulted in similar IFNγ secretion from cocultured MART-1–specific TILs (Fig. 4B). These results further suggest that

enforced MHC-I–peptide complex expression by overexpressing exogenous HLA-A2 in melanoma cells abolishes the inhibitory effect of MEX3B on tumor–T-cell recognition.

Considering all the above results, we reasoned that there may be a tumor-intrinsic defect in MEX3B-overexpressing melanoma cells resulting in their inability to be recognized by TILs, and this defect can be rescued by stable overexpression of exogenous HLA-A2. One potential mechanism is that this defect is due to downregulation of endogenous HLA-A expression in MEX3B-overexpressing cells. To test this hypothesis, we treated GFP-MEX3B–overexpressing or GFP control 2559 cells with or without INFγ, and measured the surface HLA-A2 (the main HLA-A allele expressed by 2559 cells) levels by flow cytometry. As shown in Fig. 4C, the mean fluorescence intensity (MFI) of HLA-A2 was dramatically decreased in GFP-MEX3B–overexpressing cells compared with GFP control cells, and treatment with INFγ did not reverse this phenotype. Similarly, the MFI of the surface HLA-A31 (the main HLA-A allele expressed by 2549 cells) was downregulated in 2549 cells overexpressing GFP-MEX3B compared with GFP control cells, which also held true when treated with INFγ (Supplementary Fig. S6). Taken together, these results suggest that downregulated surface HLA-A expression in MEX3B-overexpressing melanoma cells is responsible for the decreased IFNγ release from cocultured TILs.

To investigate whether MEX3B downregulates all major subclasses of MHC-I, we measured the surface levels of pan-HLA-A, B, and C in control or MEX3B-overexpressing 2559 or 2549 melanoma cells. Interestingly, we did not find any difference in pan-HLA-A, B, and C staining between control and MEX3B-overexpressing cells, regardless of the cell line tested or INFγ treatment (Supplementary Fig. S7A). We then tested whether MEX3B downregulates HLA-B or HLA-C in these cells, and again did not see any difference in HLA-B or HLA-C levels between control and MEX3B-overexpressing cells (Supplementary Fig. S7B and S7C). Therefore, it is likely that MEX3B primarily downregulates HLA-A expression in melanoma cells.

MEX3B inhibits *HLA-A* expression by binding to the 3′ UTR

We then investigated the mechanism by which MEX3B downregulates HLA-A expression. We hypothesized that MEX3B could downregulate HLA-A expression at the mRNA level. Analysis of the TCGA skin cutaneous melanoma database suggested a negative correlation between *MEX3B* and *HLA-A* mRNA expression (Fig. 5A; Pearson correlation coefficient = −0.192, P = 2.58E-005). Analysis of RNA-Seq data from a previously published cohort of patients with melanoma treated with anti–PD-1 (21) also suggested a negative association between *MEX3B* and *HLA-A* expression (Fig. 5B; Spearman correlation coefficient = −0.40, P = 0.036). Finally, qRT-PCR results suggested that overexpression of MEX3B decreased *HLA-A* mRNA expression in both 2549 and 2559 cell lines (Fig. 5C).

MEX3B is an RNA-binding protein that regulates mRNA destabilization by binding to the mRNA 3′ UTR (15). Therefore, we hypothesized that MEX3B binds to the 3′ UTR of *HLA-A* mRNA and causes *HLA-A* destabilization. To test this hypothesis, we performed a dual-luciferase reporter assay using either an ffLuc reporter construct or the same construct with its C-terminus fused with the 3′ UTR of *HLA-A2* mRNA (Fig. 5D), as well as a *Renilla* luciferase reporter construct to control for transfection efficiency. Two days after

cotransfection of these two luciferase reporter constructs with either GFP-expressing or GFP-MEX3B–expressing plasmids into 293T cells, a dual-luciferase reporter assay was performed. The relative luciferase activity resulting from the ffLuc construct fused with *HLA-A2* 3′ UTR was significantly downregulated upon overexpression of MEX3B (Fig. 5D), suggesting that MEX3B may bind to the 3′ UTR of *HLA-A2* and destabilize *HLA-A* mRNA, thereby downregulating HLA-A expression on the surface of tumor cells.

To further test this hypothesis, we also performed dual-luciferase reporter assays using a construct expressing an RNA-binding–deficient MEX3B mutant named MEX3B-mutKH, in which key residues involved in RNA binding, including Gly-83 and Gly-177 in the KH domains, are replaced with Asp (26). The relative luciferase activity resulting from the ffLuc construct fused with *HLA-A2* 3′ UTR was significantly downregulated upon transfection with wild-type MEX3B, but not with MEX3B-mutKH (Fig. 5E). This result indicates that it is the RNA-binding function of MEX3B that is responsible for the downregulation of expression of genes containing *HLA-A2* 3′ UTR.

To examine whether MEX3B directly binds to *HLA-A* mRNA, we performed a RIP assay. An MEX3B-specific antibody was used to pull down MEX3B together with its associated mRNAs, and the mRNA was recovered and subject to analysis by qRT-PCR. A mouse IgG antibody was also used as a control. In both 2549 and 2559 melanoma cells, the *HLA-A* mRNA coimmunoprecipitated with MEX3B was significantly enriched compared with those coimmunoprecipitated using mouse IgG (Fig. 5F and G), suggesting that MEX3B directly associates with *HLA-A* mRNA.

Taken together, these data indicate that MEX3B can bind to *HLA-A* mRNA 3′ UTR and destabilize the mRNA, thus downregulating HLA-A expression. The downregulated HLA-A levels may result in impaired antigen presentation on tumor cells and thus lack of recognition by T cells. However, we cannot rule out the possibility that the antigen-processing and presentation machinery (APM) is also dampened by MEX3B. To test this possibility, we analyzed the mRNA expression of multiple APM components (including B2M, TAP1, TAP2, TAPBP, CALR, CANX, PSMB8, and PSMB9) in control or MEX3B-overexpressing melanoma cells. MEX3B seems to decrease the expression of some but not all APM components, but the results are not consistent between the two cell lines (Supplementary Fig. S8A and S8B). Nevertheless, *HLA-A* expression is consistently downregulated upon MEX3B overexpression in both cell lines, suggesting this is the predominant mechanism leading to the inability of tumor cells to be recognized by T cells.

Discussion

The primary challenge of cancer immunotherapy is that a large proportion of patients do not respond to these therapies. Therefore, it is important to identify genes mediating resistance to cancer immunotherapy. In this study, we identified the RNA-binding protein MEX3B as a candidate that decreases the susceptibility of tumor cells to T-cell–mediated cytotoxicity. Furthermore, analyses of the melanoma TCGA database suggested that higher *MEX3B* expression is correlated with lower cytolytic activity and less lymphocyte infiltration in patients with melanoma. Moreover, analyses of anti–PD-1–treated melanoma patient tumor

RNA samples suggested that higher *MEX3B* expression is associated with worse response to anti–PD-1 immunotherapy. All these data suggest a role of MEX3B in mediating resistance to cancer immunotherapy.

Mechanistically, we observed that overexpression of MEX3B in melanoma cells resulted in a significant decrease in IFNγ release by cocultured autologous TILs, indicating that MEX3B impedes the recognition of tumor cells by T cells. Using MART-1 peptide pulsing and MART-1–specific TILs, we further discovered that the lack of tumor–T-cell recognition may be due in part to downregulation of surface HLA-A expression on MEX3B-overexpressing melanoma cells, as exogenous expression of HLA-A2 abolished the inhibitory effect on IFNγ release. In addition, we hypothesized that MEX3B binds to the 3′ UTR of *HLA-A2* mRNA and results in the destabilization of the mRNA. As the exogenous *HLA-A2* construct contained only the ORF and not the 3′ UTR portion, the overexpressed exogenous *HLA-A2* in tumor cells was not subject to downregulation by MEX3B and thus could reverse the phenotype of decreased IFNγ release caused by the destabilizing effect of MEX3B on endogenous *HLA-A*.

Indeed, MEX3B is a known RNA-binding protein that has been found to bind to the 3′ UTR of other mRNAs and downregulate their expression (15). For example, MEX3B destabilizes its own mRNA by binding to the 3′ LCU, which contains elements for mRNA destabilization and translational enhancement, that is, a purine-rich stretch followed by the destabilizing sequence AUUUUAUUUUA (15). It also destabilizes mRNA for FGF signaling components Syndecan 2 and Ets1b, and attenuates FGF signaling critical for neural plate patterning in *Xenopus* development (15). Furthermore, another member of the MEX3 family, MEX3C, has been found to downregulate *HLA-A2* by binding to its 3′ UTR to destabilize *HLA-A2* mRNA (27). These findings from other groups, together with our results from the dual-luciferase reporter assay using a luciferase reporter fused with the *HLA-A2* 3′ UTR and from the RIP assay showing direct binding of MEX3B to *HLA-A* mRNA, support our proposed mechanism that MEX3B binds to the *HLA-A2* 3′ UTR to destabilize the mRNA.

In summary, MEX3B mediates resistance to cancer immunotherapy by downregulating HLA-A expression on the surface of tumor cells, thus rendering the tumor cells unable to be recognized and killed by T cells. MEX3B does not seem to downregulate the expression of other subclasses of MHC-I, such as HLA-B or HLA-C. This may enable tumor cells to evade the immune attack without becoming a target for natural killer (NK) cells. The fact that downregulation of HLA-A alone in 2549 and 2559 melanoma cells resulted in lack of recognition implies that 2549 and 2559 TILs may predominantly recognize HLA-A–restricted antigen. This may also be the case for melanoma TILs in general, since HLA-A was previously found to be expressed at higher levels than HLA-B and HLA-C in melanoma (28), and the majority of well-known melanoma antigens (such as MART-1, gp100, Tyrosinase, TRP-1, TRP-2, MAGE-1, MAGE-3, etc.) are HLA-A restricted. Furthermore, we did not observe consistent alteration of expression of APM components by MEX3B, suggesting that HLA-A downregulation by MEX3B is the primary mechanism by which tumor cells become resistant to T-cell recognition and killing. Although our conclusion is based on data generated from patient-derived melanoma cell lines and their recognition and

killing by reactive TILs, we cannot rule out the possibility that there are other potential mechanisms by which MEX3B confers immunoresistance. Moreover, further investigation is needed to determine whether MEX3B also confers resistance to immunotherapy in other types of cancers beyond melanoma. Finally, little is known about upstream regulators of MEX3B, which may play important roles in tumor development. A bioinformatic search using ChampionChIP transcription factor search portal (29) has predicted several transcription factors that may regulate MEX3B expression (Supplementary Fig. S9), among which HOXA9 is known to play a role in transcriptional misregulation in cancer. In the future, the expression of these upstream regulators could be tested in patients to see whether these regulators are associated with response to immunotherapy. Nevertheless, our study has revealed the downregulation of HLA-A expression by the RNA-binding protein MEX3B as a novel mechanism of immunoresistance, which further adds to our current understanding of how tumor cells evade the immune system (10–13). Further studies will aim at identifying additional mechanisms of immunoresistance and designing novel targeted therapies to overcome immunoresistance and achieve better clinical outcomes for patients with cancer.

Supplementary Material

Refer to Web version on PubMed Central for supplementary material.

Acknowledgments

The authors would like to thank Dr. Agata Sienkiewicz and Dr. Paul Lehner from University of Cambridge and Dr. Yusuke Yamazumi and Dr. Tetsu Akiyama from University of Tokyo for providing plasmids. The authors would like to thank the past and present The University of Texas MD Anderson Cancer Center (MDACC) tumor-infiltrating lymphocyte (TIL) lab members Orenthial J. Fulbright, Arely Wahl, Esteban Flores, Shawne T. Thorsen, René J. Tavera, Renjith Ramachandran, Audrey M. Gonzalez, Christopher Toth, Seth Wardell, and Rahmatu Mansaray for generating patient-derived melanoma cells and their autologous TILs from patients with melanoma. The authors would like to thank Khalida Wani, Jared C. Malke, and Lauren E. Haydu from the Melanoma Core Lab at MDACC for gathering patient samples and doing RNA extraction. This work was supported by the NIH (R01CA184845, to P. Hwu; R01CA187076, to P. Hwu and M. A. Davies; P50CA093459, to J. A. McKenzie; and Cancer Center Support Grant P30CA016672 to the Flow Cytometry Core Facility, Monoclonal Antibody Core Facility, and Characterized Cell Line Core Facility at MDACC); by philanthropic contributions to the MDACC Melanoma Moon Shots Program; a Melanoma Research Alliance Team Science Award; the Dr. Miriam and Sheldon G. Adelson Medical Research Foundation; the Talla Family Revocable Trust; the Aim at Melanoma Foundation; Miriam and Jim Mulva Research Fund; Jurgen Sager and Transocean Melanoma Research Fund; the El Paso Foundation for Melanoma Research; and also by the Cancer Prevention and Research Institute of Texas (CPRIT; RP170401, to P. Hwu; and RP140106 and RP170067, to J.A. McKenzie).

The costs of publication of this article were defrayed in part by the payment of page charges. This article must therefore be hereby marked *advertisement* in accordance with 18 U.S.C. Section 1734 solely to indicate this fact.

References

1. Lizee G, Overwijk WW, Radvanyi L, Gao J, Sharma P, Hwu P. Harnessing the power of the immune system to target cancer. Annu Rev Med 2013;64:71–90. [PubMed: 23092383]
2. Brahmer J, Reckamp KL, Baas P, Crino L, Eberhardt WE, Poddubskaya E, et al. Nivolumab versus docetaxel in advanced squamous-cell non-small-cell lung cancer. N Engl J Med 2015;373:123–35. [PubMed: 26028407]
3. Hodi FS, O'Day SJ, McDermott DF, Weber RW, Sosman JA, Haanen JB, et al. Improved survival with ipilimumab in patients with metastatic melanoma. N Engl J Med 2010;363:711–23. [PubMed: 20525992]

4. Pardoll DM. The blockade of immune checkpoints in cancer immunotherapy. Nat Rev Cancer 2012;12:252–64. [PubMed: 22437870]
5. Postow MA, Chesney J, Pavlick AC, Robert C, Grossmann K, McDermott D, et al. Nivolumab and ipilimumab versus ipilimumab in untreated melanoma. N Engl J Med 2015;372:2006–17. [PubMed: 25891304]
6. Radvanyi LG, Bernatchez C, Zhang M, Fox PS, Miller P, Chacon J, et al. Specific lymphocyte subsets predict response to adoptive cell therapy using expanded autologous tumor-infiltrating lymphocytes in metastatic melanoma patients. Clin Cancer Res 2012;18:6758–70. [PubMed: 23032743]
7. Robbins PF, Kassim SH, Tran TL, Crystal JS, Morgan RA, Feldman SA, et al. A pilot trial using lymphocytes genetically engineered with an NY-ESO-1-reactive T-cell receptor: long-term follow-up and correlates with response. Clin Cancer Res 2015;21:1019–27. [PubMed: 25538264]
8. Robbins PF, Morgan RA, Feldman SA, Yang JC, Sherry RM, Dudley ME, et al. Tumor regression in patients with metastatic synovial cell sarcoma and melanoma using genetically engineered lymphocytes reactive with NY-ESO-1. J Clin Oncol 2011;29:917–24. [PubMed: 21282551]
9. Topalian SL, Sznol M, McDermott DF, Kluger HM, Carvajal RD, Sharfman WH, et al. Survival, durable tumor remission, and long-term safety in patients with advanced melanoma receiving nivolumab. J Clin Oncol 2014;32:1020–30. [PubMed: 24590637]
10. Peng W, Chen JQ, Liu C, Malu S, Creasy C, Tetzlaff MT, et al. Loss of PTEN promotes resistance to T cell-mediated immunotherapy. Cancer Discov 2016;6:202–16. [PubMed: 26645196]
11. Gao J, Shi LZ, Zhao H, Chen J, Xiong L, He Q, et al. Loss of IFN-gamma pathway genes in tumor cells as a mechanism of resistance to anti-CTLA-4 therapy. Cell 2016;167:397–404. [PubMed: 27667683]
12. Zaretsky JM, Garcia-Diaz A, Shin DS, Escuin-Ordinas H, Hugo W, Hu-Lieskovan S, et al. Mutations associated with acquired resistance to PD-1 blockade in melanoma. N Engl J Med 2016;375:819–29. [PubMed: 27433843]
13. Spranger S, Bao R, Gajewski TF. Melanoma-intrinsic beta-catenin signalling prevents anti-tumour immunity. Nature 2015;523:231–5. [PubMed: 25970248]
14. Buchet-Poyau K, Courchet J, Le Hir H, Seraphin B, Scoazec JY, Duret L, et al. Identification and characterization of human Mex-3 proteins, a novel family of evolutionarily conserved RNA-binding proteins differentially localized to processing bodies. Nucleic Acids Res 2007;35:1289–300. [PubMed: 17267406]
15. Takada H, Kawana T, Ito Y, Kikuno RF, Mamada H, Araki T, et al. The RNA-binding protein Mex3b has a fine-tuning system for mRNA regulation in early Xenopus development. Development 2009;136:2413–22. [PubMed: 19542354]
16. Yang Y, Wang SY, Huang ZF, Zou HM, Yan BR, Luo WW, et al. The RNA-binding protein Mex3B is a coreceptor of Toll-like receptor 3 in innate antiviral response. Cell Res 2016;26:288–303. [PubMed: 26823206]
17. Zhu S, Wang G, Lei X, Flavell RA. Mex3B: a coreceptor to present dsRNA to TLR3. Cell Res 2016;26:391–2. [PubMed: 26940660]
18. Forget MA, Malu S, Liu H, Toth C, Maiti S, Kale C, et al. Activation and propagation of tumor-infiltrating lymphocytes on clinical-grade designer artificial antigen-presenting cells for adoptive immunotherapy of melanoma. J Immunother 2014;37:448–60. [PubMed: 25304728]
19. He L, Hakimi J, Salha D, Miron I, Dunn P, Radvanyi L. A sensitive flow cytometry-based cytotoxic T-lymphocyte assay through detection of cleaved caspase 3 in target cells. J Immunol Methods 2005;304:43–59. [PubMed: 16076473]
20. The Cancer Genome Atlas Network. Genomic classification of cutaneous melanoma. Cell 2015;161:1681–96. [PubMed: 26091043]
21. Hugo W, Zaretsky JM, Sun L, Song C, Moreno BH, Hu-Lieskovan S, et al. Genomic and transcriptomic features of response to anti-PD-1 therapy in metastatic melanoma. Cell 2016;165:35–44. [PubMed: 26997480]
22. Johannessen CM, Boehm JS, Kim SY, Thomas SR, Wardwell L, Johnson LA, et al. COT drives resistance to RAF inhibition through MAP kinase pathway reactivation. Nature 2010;468:968–72. [PubMed: 21107320]

23. Cerami EG, Gross BE, Demir E, Rodchenkov I, Babur O, Anwar N, et al. Pathway Commons, a web resource for biological pathway data. Nucleic Acids Res 2011;39(Database issue):D685–90. [PubMed: 21071392]

24. Rooney MS, Shukla SA, Wu CJ, Getz G, Hacohen N. Molecular and genetic properties of tumors associated with local immune cytolytic activity. Cell 2015;160:48–61. [PubMed: 25594174]

25. Kawakami Y, Eliyahu S, Sakaguchi K, Robbins PF, Rivoltini L, Yannelli JR, et al. Identification of the immunodominant peptides of the MART-1 human melanoma antigen recognized by the majority of HLA-A2-restricted tumor infiltrating lymphocytes. J Exp Med 1994;180:347–52. [PubMed: 7516411]

26. Yamazumi Y, Sasaki O, Imamura M, Oda T, Ohno Y, Shiozaki-Sato Y, et al. The RNA binding protein Mex-3B is required for IL-33 induction in the development of allergic airway inflammation. Cell Rep 2016;16:2456–71. [PubMed: 27545879]

27. Cano F, Bye H, Duncan LM, Buchet-Poyau K, Billaud M, Wills MR, et al. The RNA-binding E3 ubiquitin ligase MEX-3C links ubiquitination with MHC-I mRNA degradation. EMBO J 2012;31:3596–606. [PubMed: 22863774]

28. Marincola FM, Shamamian P, Simonis TB, Abati A, Hackett J, O'Dea T, et al. Locus-specific analysis of human leukocyte antigen class I expression in melanoma cell lines. J Immunother Emphasis Tumor Immunol 1994;16: 13–23. [PubMed: 8081556]

29. Champion ChiP Transcription Factor Search Portal. 2012–05–12 ed. Valencia (CA): Qiagen; c2000.

Translational Relevance

Cancer immunotherapy has shown promising clinical outcomes in many patients, but some patients fail to respond. Therefore, new strategies are needed to overcome resistance, and understanding the molecular mechanisms of resistance to immunotherapy is of critical importance. In this study, using patient-derived melanoma cells and autologous tumor-infiltrating lymphocytes (TIL), we revealed the downregulation of HLA-A expression by the RNA-binding protein MEX3B as a novel mechanism for tumor cells to evade attack by the immune system. Furthermore, analyses of The Cancer Genome Atlas (TCGA) melanoma database suggested that higher *MEX3B* expression is correlated with lower cytolytic activity and less lymphocyte infiltration in patients with melanoma. Moreover, analyses of anti–PD-1–treated melanoma patient tumor samples suggested that higher *MEX3B* expression is associated with resistance to anti–PD-1 immunotherapy. Our findings have the potential to lead to the development of therapeutic strategies targeting MEX3B in the hope of overcoming immunoresistance and achieving better clinical outcomes for patients with melanoma treated with immunotherapy.

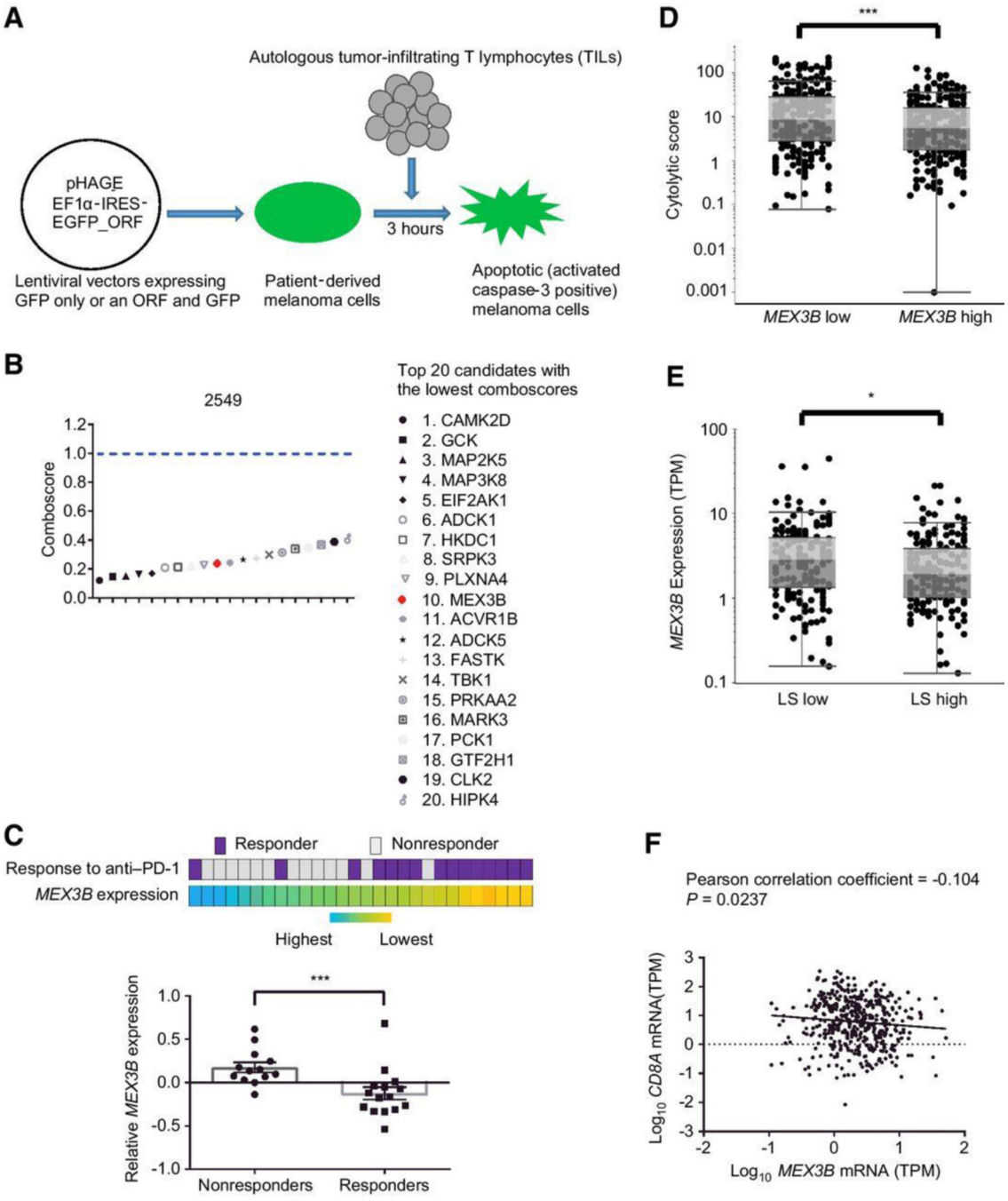

Figure. 1. MEX3B was identified from an ORF screen to mediate resistance to T-cell–mediated tumor cytotoxicity.

MEX3B was identified from an ORF screen to mediate resistance to T-cell–mediated tumor cytotoxicity. **A**, Schematic illustration of the ORF screen in patient-derived melanoma cells. **B**, The comboscore was calculated using the following formula: $[(\text{Apoptosis}_{ORF+TILs} - \text{Apoptosis}_{ORF})/(\text{Apoptosis}_{GFP+TILs} - \text{Apoptosis}_{GFP})]^2$. The top 20 candidates with the lowest comboscores are shown. MEX3B is one of these top candidates (highlighted in red). **C**, The relative mRNA expression of *MEX3B* (using Z score as the readout) from

15 responders and 13 nonresponders to anti–PD-1 immunotherapy was analyzed based on the RNA-Seq data from a published anti–PD-1–treated melanoma patient cohort. Top: The *MEX3B* Z scores of all samples are ranked from highest to lowest and represented in gradually changing colors from blue to orange. Each column represents the response information (purple, responder; gray, nonresponder) and the *MEX3B* mRNA expression (blue, high; orange, low) of each patient. Bottom: The Z scores (as a readout for relative *MEX3B* expression) of each responder or nonresponder are shown. ***, $P < 0.001$ by Mann–Whitney test. **D**, TCGA analysis of the correlation of the expression of *MEX3B* with cytolytic score in patients with skin cutaneous melanoma. *MEX3B* high (above median expression, $n = 236$) group: median cytolytic score is 5.66, with an SD of 19.05. *MEX3B* low (below median expression, $n = 236$) group: median cytolytic score is 8.41, with an SD of 41.80. ***, $P < 0.001$ by Mann–Whitney test. **E**, TCGA analysis of the correlation of lymphocyte score (LS) with the expression of *MEX3B* in patients with melanoma. LS low (scores 0, 1, and 2; $n = 167$) group: median *MEX3B* expression is 2.87, with an SD of 5.69. LS high (scores 3, 4, 5, and 6; $n = 163$) group: median MEX3B expression is 1.93, with an SD of 3.42. *, $P < 0.05$ by Mann–Whitney test. **F**, TCGA analysis of the correlation between the expression of *MEX3B* and *CD8A*. Each dot represents $\log_{10}$-transformed mRNA expression of each tumor sample ($n = 472$). Pearson correlation coefficient = −0.104, $P = 0.0237$.

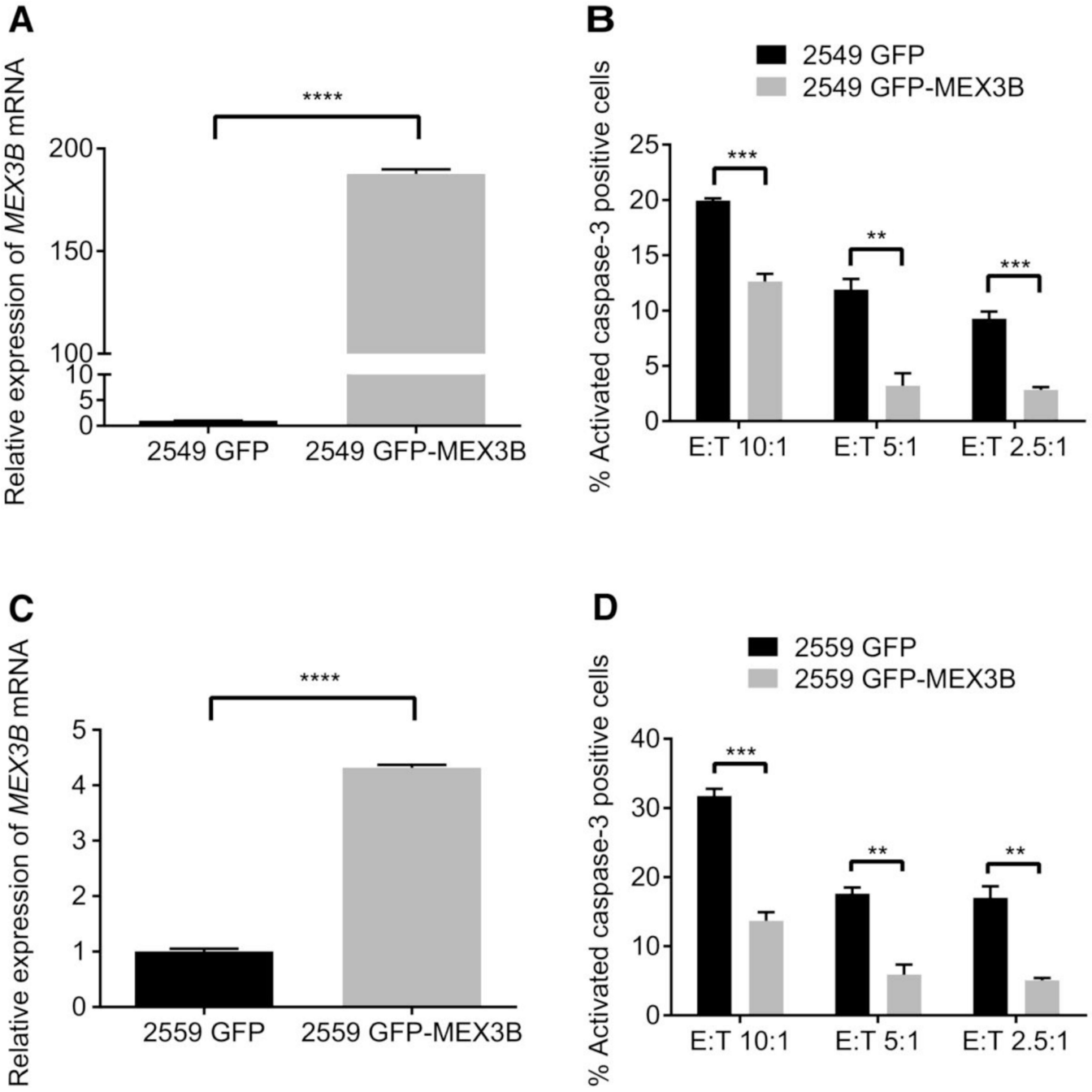

Figure 2. Overexpression of MEX3B in tumor cells decreases their susceptibility to T-cell–mediated cytotoxicity. qRT-PCR validation of overexpression of MEX3B in 2549 (A) and 2559 (C) melanoma cells.

Overexpression of MEX3B in tumor cells decreases their susceptibility to T-cell–mediated cytotoxicity. qRT-PCR validation of overexpression of MEX3B in 2549 (**A**) and 2559 (**C**) melanoma cells. GFP-MEX3B-overexpressing or GFP control 2549 (**B**) or 2559 (**D**) melanoma cells were incubated with autologous 2549 TILs (**B**) or 2559 TILs (**D**) at different E:T ratios for 3 hours, followed by quantification of apoptosis by flow cytometry analysis

of activated caspase-3. Data are represented as mean ± SEM. **, $P < 0.01$; ***, $P < 0.001$; ****, $P < 0.0001$ by Student *t* test.

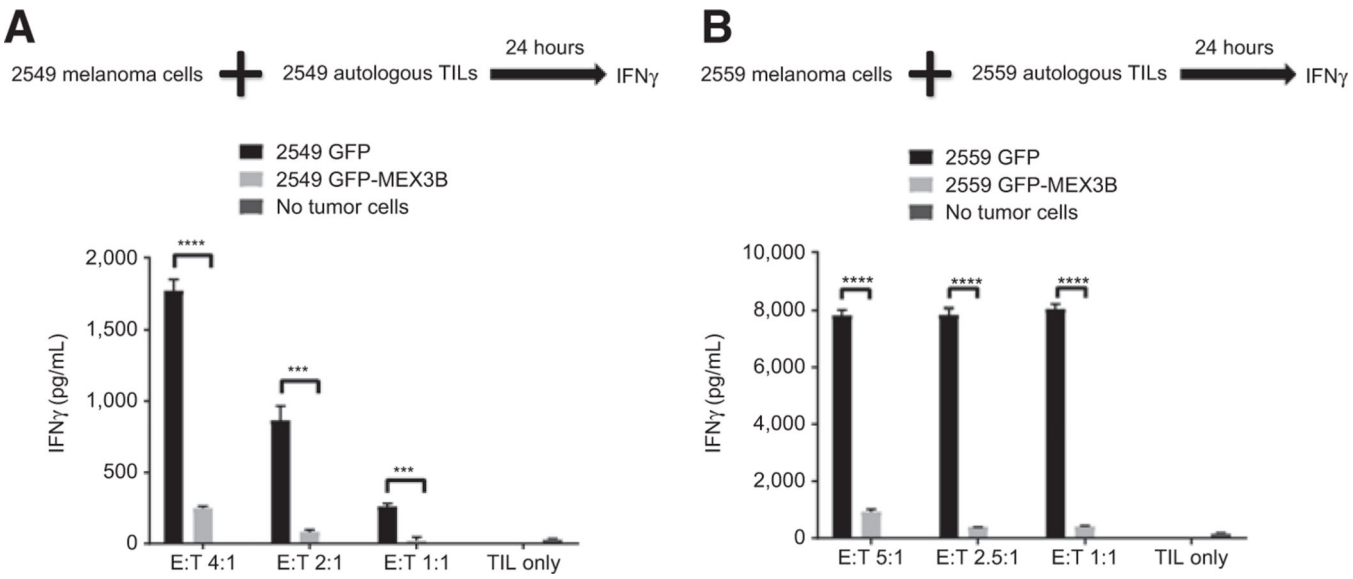

Figure 3. Overexpression of MEX3B in melanoma cells decreases IFNγ release from autologous TILs.

A, GFP-MEX3B–overexpressing or GFP control 2549 cells were incubated with autologous 2549 TILs at different E:T ratios for 24 hours, followed by measurement of IFNγ levels in supernatants by ELISA. **B**, GFP-MEX3B–overexpressing or GFP control 2559 cells were incubated with autologous 2559 TILs at different E:T ratios for 24 hours, followed by measurement of IFNγ levels in supernatants by ELISA. Data are represented as mean SEM. ***, $P < 0.001$; ****, $P < 0.0001$ by Student *t* test.

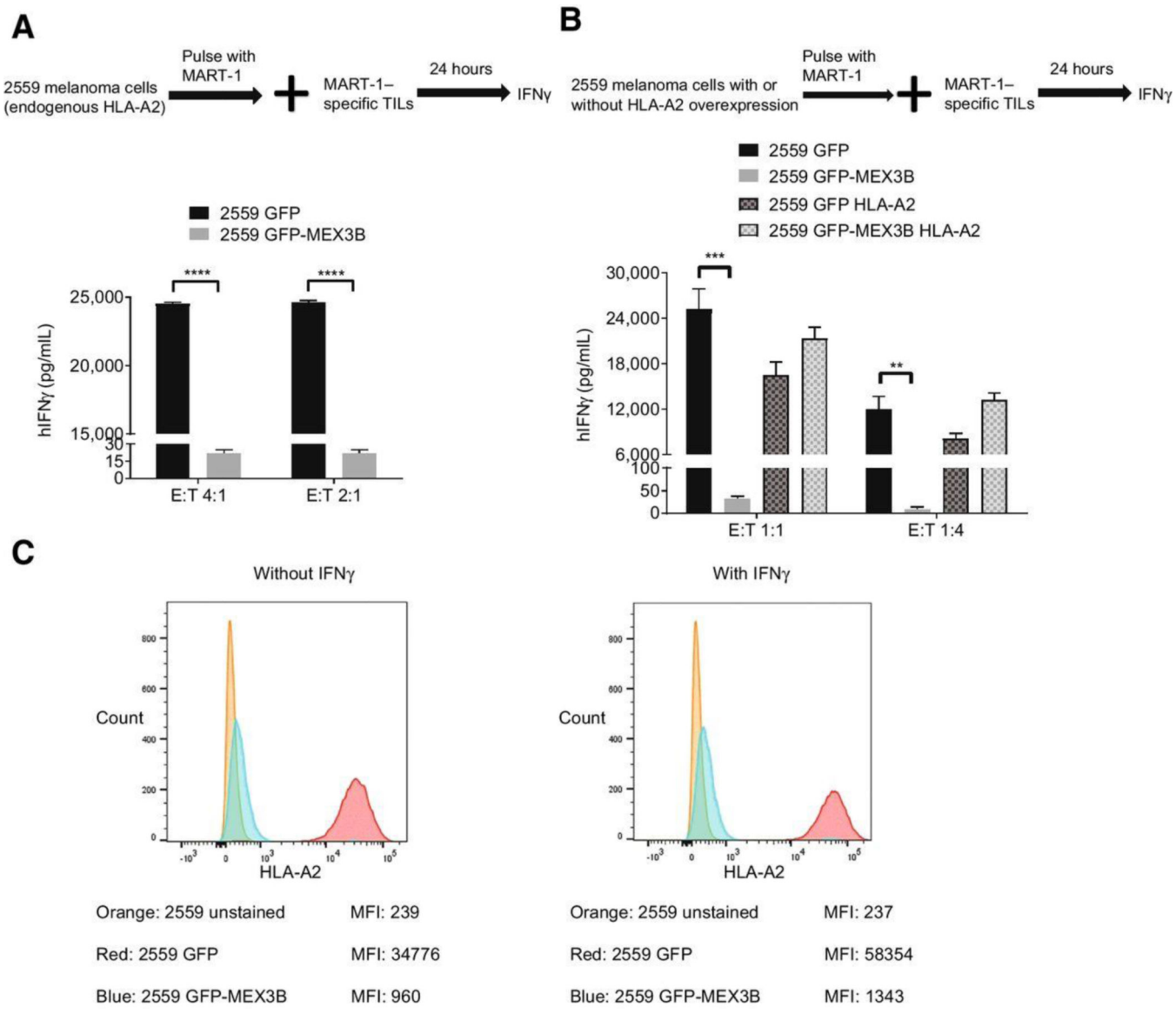

Figure 4. Decreased surface HLA-A levels in MEX3B-overexpressing melanoma cells is responsible for the decreased IFNγ release from TILs.

A, GFP-MEX3B–overexpressing or GFP control 2559 cells were pulsed with MART-1 for 1 hour and incubated with MART-1–specific TILs at different E:T ratios for 24 hours, followed by measurement of IFNγ levels in supernatants by ELISA. **B**, GFP-MEX3B–overexpressing or GFP control 2559 cells, as well as those cells overexpressing exogenous HLA-A2, were pulsed with MART-1 for 1 hour and incubated with MART-1–specific TILs at different E:T ratios for 24 hours, followed by measurement of IFNγ levels in supernatants by ELISA. Data are represented as mean ± SEM. **, $P < 0.01$; ***, $P < 0.001$; ****, $P < 0.0001$ by Student *t* test. **C**, GFP-MEX3B–overexpressing or GFP control 2559 cells were treated with or without IFNγ for 24 hours and stained for HLA-A2, followed by flow cytometry analysis. The representative histograms of each cell line and unstained control, as well as their mean fluorescent intensity (MFI) of HLA-A2, are shown. This graph is representative of three independent experiments.

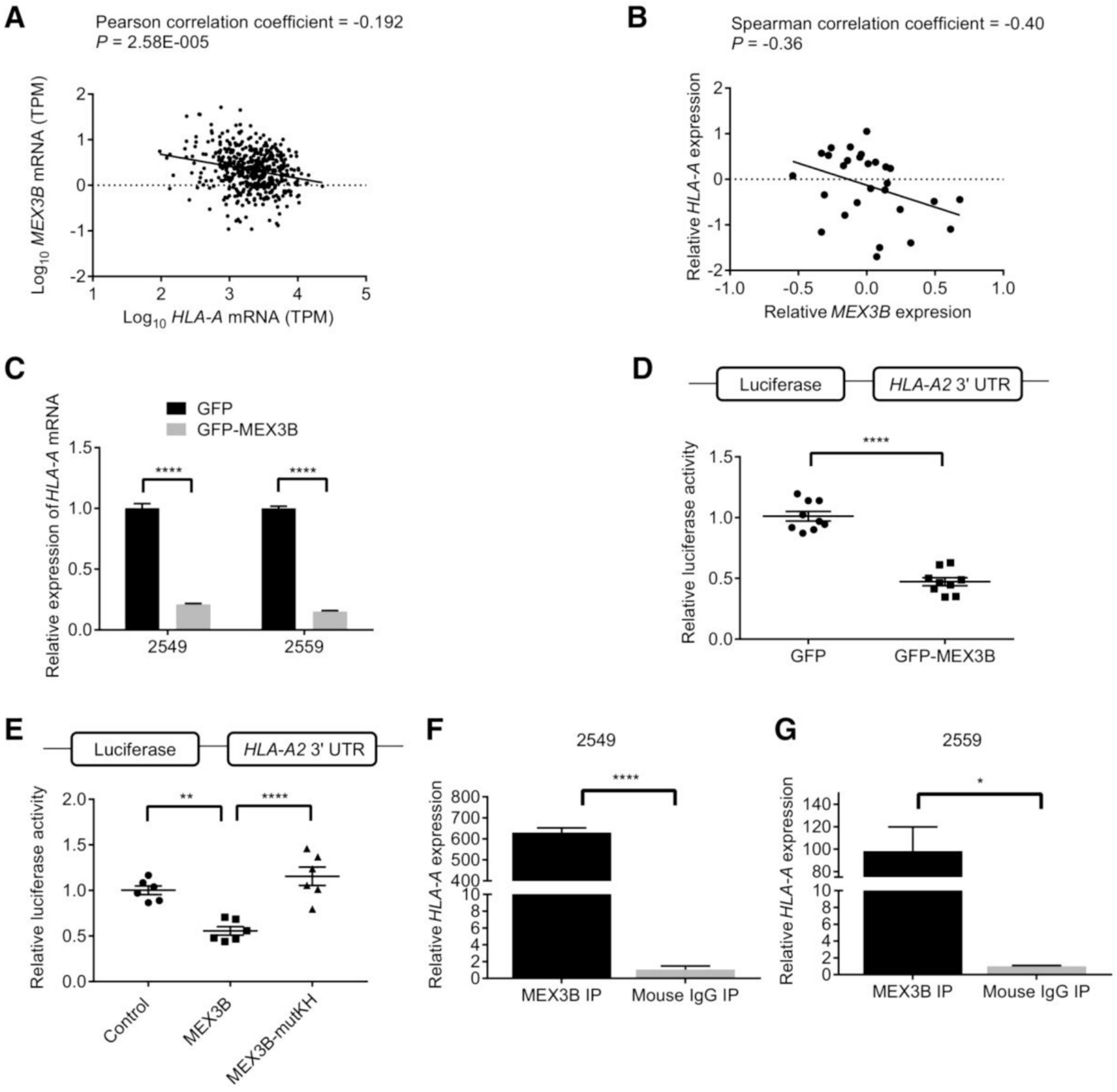

Figure 5. Overexpression of MEX3B inhibits HLA-A by binding to the 3′ UTR.

A, The correlation between MEX3B and HLA-A mRNA expression in the skin cutaneous melanoma TCGA database is shown. Overexpression of MEX3B inhibits HLA-A by binding to the 3′ UTR. **B**, The correlation between *MEX3B* and *HLA-A* mRNA expression based on the RNA-Seq data from a published anti–PD-1–treated melanoma patient cohort that is the same as in Fig. 1C. Each dot represents relative mRNA expression of each tumor sample ($n = 28$). **C**, qRT-PCR analysis of *HLA-A* mRNA expression in GFP-MEX3B–overexpressing or GFP control 2549 or 2559 cells. **D** and **E**, Dual-luciferase reporter assays were performed using a ffLuc reporter construct or the same construct with its C-

terminus fused with the 3′ UTR of *HLA-A2* mRNA as well as a *Renilla* luciferase reporter construct to control the transfection efficiency. These two luciferase reporter constructs, together with GFP-expressing or GFP-MEX3B–expressing plasmids (**D**) or pCDNA3.1 vector or pCDNA3.1-MEX3B (wild type) or pCDNA3.1-MEX3B-mutKH plasmids (**E**), were transiently transfected into 293T cells. Two days after transfection, dual-luciferase reporter assays were performed. The relative luciferase activity (from the *HLA-A2* 3′ UTR–containing ffLuc construct relative to the control ffLuc construct) in cells transfected with GFP-expressing or GFP-MEX3B–expressing plasmids was compared by Student *t* test (**D**). The experiment was done in triplicate each time (i.e., for each combination of plasmids, three wells of 293T cells were transfected) and repeated three independent times. Similarly, the relative luciferase activity in cells transfected with pCDNA3.1 vector, pCDNA3.1-MEX3B (wild type), or pCDNA3.1-MEX3B-mutKH plasmids was compared by ANOVA plus the Tukey multiple comparison test (**E**). The experiment was done in triplicate each time and repeated two independent times. Each dot represents the relative luciferase activity of one well from one experiment. **F** and **G**, A RIP assay was performed on 2549 (**F**) or 2559 (**G**) melanoma cells. Cell lysates were immunoprecipitated (IP) with mouse anti-MEX3B antibody or mouse IgG as a control. Coimmunoprecipitated RNA was recovered, and qRT-PCR was performed to amplify *HLA-A*. MEX3B-associated *HLA-A* levels were normalized to control mouse IgG–associated *HLA-A* levels. Data are represented as mean ± SEM. *, $P < 0.05$; **, $P < 0.01$; ****, $P < 0.0001$ by Student *t* test.